Ultrafast photoresponse of metallic and semiconducting single-wall carbon nanotubes

Randy J. Ellingson, Chaiwat Engtrakul, Marcus Jones, Monica Samec, Garry Rumbles, Arthur J. Nozik, and Michael J. Heben
Center for Basic Sciences, National Renewable Energy Laboratory, Golden, Colorado 80401, USA
(Received 26 November 2003; revised manuscript received 22 November 2004; published 31 March 2005)

Utilizing a transient absorption (TA) technique based on a chirp-corrected broadband probe, we have studied the ultrafast photoresponse of dispersed HiPco single-wall carbon nanotubes (SWNTs) over the range of 440–1050 nm for excitation in the range of 430–1700 nm. While both metallic and semiconducting SWNTs show transient bleaching at their M_{11} and S_{11} energies for excitation above these energies, metallic SWNTs uniquely exhibit a photoresponse to sub-M_{11} excitation. We observe a TA spectral response for metallic SWNTs which is consistent with thermal broadening of the M_{11} transition bands. In contrast to metallic SWNTs, specific semiconducting SWNTs exhibit transparency for sub-S_{11} excitation, in accord with the expected zero density of states below the first interband transition. We report the observation of a long-lived ($\tau > 1$ ns) transient bleach component for three semiconducting SWNT species.

DOI: 10.1103/PhysRevB.71.115444 PACS number(s): 73.22.−f, 71.35.−y, 73.21.−b

INTRODUCTION

The unique structural and electronic properties of single-wall carbon nanotubes (SWNTs) have attracted considerable attention for a variety of technological applications including hydrogen storage,[1] field emission displays,[2,3] and composite materials.[4,5] We seek to explore SWNTs as photoactive agents in solar energy conversion, and present here research undertaken to explore the ultrafast photophysics of dispersed SWNTs. Raman, absorption, and photoluminescence (PL) spectroscopies have provided extensive characterization of specific SWNT species of both semiconducting and metallic electronic structure.[6–8] Recent time-resolved studies of SWNT charge carrier dynamics[9–18] have focused primarily on the transient response of semiconducting SWNTs. Many questions remain regarding the nature and dynamics of charge carrier relaxation, recombination, separation, and transport. We present results of ultrafast transient absorption (TA) studies of dispersed SWNTs which show distinctly different behavior for semiconducting and metallic SWNTs. Carrier heating due to photoexcitation,[17] followed by thermal equilibration with the lattice, dominate the ultrafast photophysics of metallic SWNTs. Unlike metallic SWNTs, semiconducting SWNTs exhibit transparency for energies below the lowest-energy interband transition, consistent with a true zero density of states (DOS) within the band gap. Semiconducting SWNTs also show a long-lived photoinduced bleach consistent with state filling of the lowest-energy interband transition.

Synthesis yields bundles of SWNTs in strong van der Waals contact with one another. Samples of bundled SWNTs are characterized by a low level of structure in steady-state absorption spectra, and an absence of semiconductor SWNT PL due to quenching by cobundled metallic SWNTs. Ultrafast pump-probe studies of such bundled SWNTs indicate short-lived charge carriers, with characteristic recombination times of $\lesssim 5$ ps.[9–11] In contrast, optical studies of SWNTs dispersed as sodium dodecyl sulfate–(SDS-)encased micelles in water show clear interband transition features in the absorption spectrum, and corresponding band-gap photoluminescence.[6] Wavelength-degenerate pump-probe studies in the band-gap region of isolated SWNTs have been reported;[12,14] in addition to a fast initial $\lesssim 1$ ps absorption bleach decay, these studies report a slower-decay component of as long as 30 ps which they attributed to interband carrier recombination in isolated SWNTs. The two-color pump-probe work of Huang *et al.* reports transient bleach signals of more than 100 ps lifetime.[13] Ma *et al.* applied TA as well as time-resolved PL techniques to study isolated high pressure CO (HiPco) SWNTs, and found evidence that some photoexcited carriers follow routes to trap states rather than to emissive states,[15] a result with significant implications for determination of the photoluminescence quantum yield.

Here, we present ultrafast transient absorption studies of a solution of dispersed, photoluminescent HiPco SWNTs using a tunable, pulsed excitation source and a broadband probe. The spectrally broad probe permits observation of the TA signal over the range of 440–1050 nm (1.2–2.8 eV), and reveals richly featured TA spectra. A high degree of correspondence is observed between the linear absorption spectrum and the spectral dependence of the TA response. In particular, photoexcitation produces transient spectra with photoinduced bleaching at energies corresponding to peaks in the linear absorption spectrum. An independently tunable pump permits excitation either above or below the probed first interband transitions, and allows distinction between spectral features corresponding to semiconducting and metallic SWNTs. Metallic SWNTs show a TA response when excited either above or below their lowest interband transition; semiconducting SWNTs, on the other hand, show a dramatically weakened response to sub-band-gap excitation, in accord with their expected gap in the DOS. We observe a consistently fast rise time of $\lesssim 100$ fs for the TA signal at the first transition energy. Following the ultrafast relaxation, recombination dynamics indicate density-dependent carrier lifetimes ranging from a few hundred femtoseconds to greater than 1 ns.

EXPERIMENT

Following closely a previously published procedure,[6] HiPco (Ref. 19) SWNTs obtained from Carbon Nanotech-

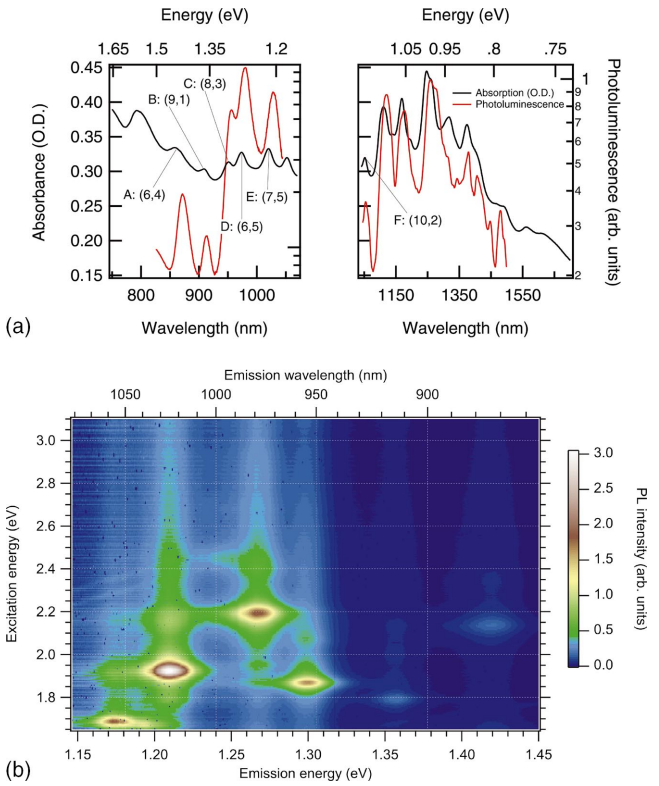

FIG. 1. (Color) (a) Absorption and photoluminescence spectra for HiPco SWNTs dispersed in D_2O with SDS surfactant. Emission spectra were measured using 532 nm laser excitation. Labeled features correspond to semiconducting SWNT emission peaks. (b) Near-infrared photoluminescence excitation spectrum, detected using a liquid-nitrogen-cooled CCD.

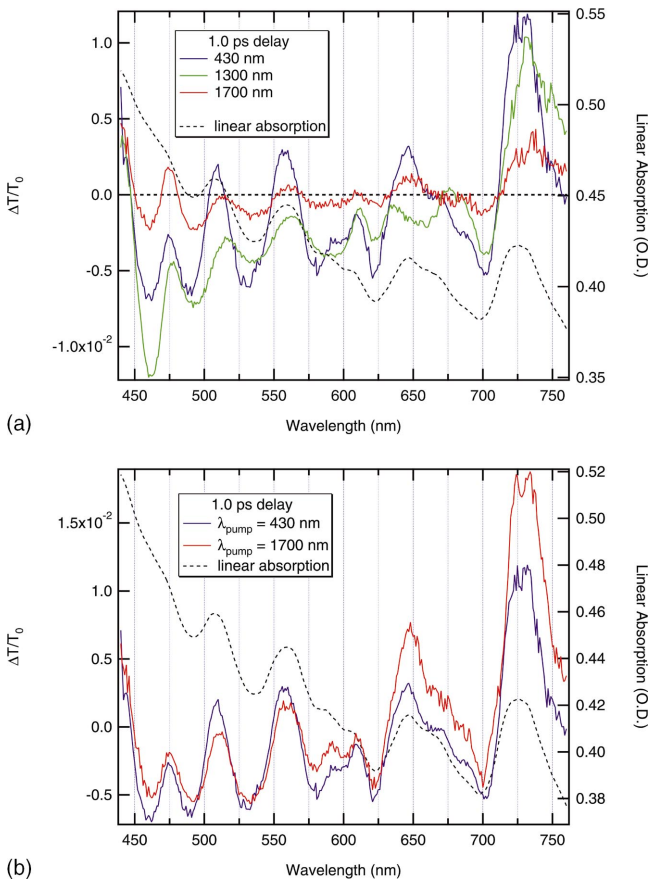

FIG. 2. (Color) (a) Transient absorption spectra for excitation at 430, 1300, and 1700 nm, acquired at 1.0 ps delay relative to peak signal and for an absorbed photon density held constant at 2.5×10^{14} cm^{-2}. The dotted line shows the linear absorption spectrum. (b) Transient absorption spectra for 430 and 1700 nm, at 1.0 ps delay, for which the excitation intensity was adjusted to achieve the same total excitation pulse energy absorbed (1.15×10^{-4} J/cm^2).

nologies were dispersed in deuterium oxide (D_2O) at pH 7 by sonication in the presence of sodium dodecyl sulfate, and spun in an ultracentrifuge (Beckman Coulter, Optima XL-100K) at 26 000 rpm ($g \cong 90\,000$) for 4 h using a swing bucket rotor (SW-28). Deuterium oxide was employed to improve the solvent transparency for absorption and emission measurements. Using similar procedures and starting with sonication of the raw HiPco material at a concentration of 300 mg/l, Moore *et al.*[20] determined a dispersion process yield from the differential sedimentation technique of 9.9 mg/l. Our starting material concentration was 500 mg/l and we therefore estimate that our final solubilized SWNT concentration is ~17 mg/l. Linear absorption was measured using a 1 mm path-length solution and a Cary 500 spectrometer by referencing absorption to a solution with 1% by weight of SDS in D_2O. We note that the spectral features evident in our absorption and emission spectra match well with those published elsewhere for solutions of SDS-encased HiPco SWNTs.[6,21] Photoluminescence spectra [Fig. 1(a)] were measured using 150 mW of 532 nm continuous wave laser excitation, and a spot diameter of ~200 μm. Emission was collected at a right angle, collimated, focused into a Spex Triax 190 spectrometer, and detected using either an InGaAs photodiode operating at 77 K (emission between 1000 and 1500 nm) or a standard liquid-nitrogen-cooled charge-coupled device (CCD) (800–1100 nm). Photoluminescence excitation (PLE) spectra [Fig. 1(b)] were recorded using a Fluorlog-3 (JY Horiba), coupled to a liquid-nitrogen-cooled CCD. Tunable excitation for PLE was achieved using a Xe arc lamp dispersed by a double monochrometer. All steady-state and time-resolved measurements were performed with the sample at room temperature.

Transient absorption measurements were conducted using a previously described system[22] based on a 1 kHz ultrafast regeneratively amplified Ti:sapphire laser (Clark CPA-2001) pumping a tunable optical parametric amplifier (Light Conversion Topas). We employ interference bandpass filters on the pump beam to ensure spectral purity; pump pulse widths are typically ~125 fs. At the longest excitation wavelength of 1700 nm, the 1 mm path-length sample of SWNTs in D_2O exhibited a ratio of SWNT to solvent absorption of 8.5, showing that 88% of the excitation light is absorbed by SWNTs while 12% is absorbed by the D_2O. The probe pulses were generated as a white light continuum by focusing a few milliwatts of the 775 nm Ti:sapphire laser pulse train onto a 2 mm sapphire window; the probe beam spectrum extended from ~440 to 1050 nm (1.18 to 2.82 eV). Transient absorption measurements probe the photoinduced

change in transmission either spectrally at fixed delay, or temporally by scanning the delay at fixed wavelength. Spectral TA measurements employed chirp correction[23] and were made at a delay of 1.0 ps relative to the signal peak. Unless otherwise noted, the photoexcitation intensity was adjusted to maintain the per pulse absorbed photon density at 2.5×10^{14} cm^{-2}.

RESULTS AND DISCUSSION

SWNTs in the diameter range of ~0.6 to 2.5 nm exhibit a quantum-wire-like DOS, with Van Hove singularities (VHSs) appearing as narrow peaks, or spikes, in the valence and conduction bands. The absorption spectrum of a distribution of nanotubes shows features arising from electronic transitions between the VHSs of both metallic and semiconducting SWNTs.[21] We refer to the lowest two transitions between VHSs in the valence and conduction bands of semiconducting SWNTs as S_{11} and S_{22}, and to those of the first transition in metallic SWNTs as M_{11}. Figure 1(a) shows representative linear absorption and steady-state emission spectra ($\lambda_{\text{excitation}} = 532$ nm) for our dispersed HiPco material over the range of the S_{11} transitions for the semiconducting SWNTs in our distribution (~0.75 to 1.42 eV). The high degree of correlation between the linear absorption and emission spectra indicates significant quantities of dispersed, isolated SWNTs.[6] Band-gap emission is redshifted by ~5–10 meV, consistent with the magnitude of the emission redshift expected for interactions between photoexcited SWNTs and the surfactant-solution environment.[20]

The lineal photoexcitation density, averaged over the specific nanotube species in our sample, can be estimated for our TA measurements as follows. For a solubilized SWNT concentration of ~17 mg/l, and a lineal mass density of 2.06×10^{-18} g/μm for the (11,0) nanotube representative of the average tube diameter in the HiPco sample, the areal density of nanotube length in a 1 mm pathlength cuvette is 8.2×10^{11} μm/cm^2. Using values from the linear absorption spectrum, we compute values for the *average* absorption cross section per unit length of nanotube, σ_a, at specific excitation energies. As examples, we find $\sigma_a(1.24\ \text{eV}) = 9.9 \times 10^{-13}$ cm^2/μm and $\sigma_a(2.92\ \text{eV}) = 1.8 \times 10^{-12}$ cm^2/μm. Applying simple geometrical considerations, the (11,0) nanotube, of 0.87 nm diameter, yields a physical cross section of 8.7×10^{-12} cm^2/μm. Based on our per pulse absorbed photon density of 2.5×10^{14} photons/cm^2, we estimate an *average* excitation density of 300 photons absorbed per micrometer length of nanotube with each laser pulse. Compared to that which would be observed for a sample of pure, isolated SWNTs, the presence of impurities would increase the sample extinction, while any residual bundles would reduce the sample extinction; we have not attempted to quantify these effects, and therefore do not account for them in our calculations. While sample polydispersity complicates the application of these order-of-magnitude calculations, an estimate of the excitation density provides insight into possible carrier-carrier interactions and thermal effects.

Numerous studies have addressed the predicted and measured electronic band structure of SWNTs arising from their circumferential and axial periodic structure.[24–29] Metallic SWNTs, apart from a ~30–100 meV pseudogap around E_F for zigzag nanotubes,[30] exhibit a nonzero DOS for energies below the M_{11} transition. In contrast, ideal semiconducting SWNTs display a true zero DOS for energies below their S_{11} transitions.

Figure 2(a) shows TA spectra at 1 ps delay for pump wavelengths of 430, 1300, and 1700 nm, holding the absorbed photon density constant, at 2.5×10^{14} cm^{-2}. Tuning the pump wavelength to the red while maintaining a constant absorbed photon density results in a decrease in total pump pulse energy delivered to the sample at longer wavelengths, varying as $1/\lambda_{\text{pump}}$. The 440–760 nm spectral region ("visible probe region") is known to include S_{22} transitions for semiconducting SWNTs as well as M_{11} transitions for metallic HiPco SWNTs. Furthermore, we note that semiconducting SWNTs in the lowest S_{11} excited state may exhibit a transient absorption signal at the S_{22} energy.[14] Photoexcitation of SWNTs does not require resonance with S_{11} or S_{22} transitions,[16] as evidenced by the emission profile of SWNTs for 532 nm excitation [Fig. 1(a)] as well as by the emission visible as vertical streaks within the excitation spectrum [Fig. 1(b)]. When pumping at 430 nm, we excite all SWNT species within the sample since $h\nu_{\text{pump}} > S_{11}$ for all semiconducting SWNTs, and metallic SWNTs are excited either by absorption above the M_{11}, or via sub-M_{11} absorption.[11,17] Tuning to $\lambda_{\text{pump}} = 1300$ nm, we expect to exclude from excitation those semiconducting SWNT species with E_{11} transitions corresponding to $\lambda_{11} < 1300$ nm. However, the spectra for excitation at 430 and 1300 nm [Fig. 2(a)] are remarkably similar, showing that we have not removed any significant TA features corresponding to S_{22} transitions. Tuning the pump further to the red at $\lambda_{\text{pump}} = 1700$ nm, the TA spectrum again appears largely unchanged, except for a further reduction in signal amplitude. The 1700 nm excitation energy (0.73 eV) lies below the S_{11} transitions for virtually all SWNTs in the HiPco sample, as evidenced by the absorption spectrum [Fig. 1(a)]. While we expect the 1700 nm pump to excite the few large-diameter semiconducting nanotube species with $E_{11} < 0.73$ eV, we remarkably also observe a significant TA response in the M_{11} region of metallic SWNTs.

For HiPco SWNTs, the prominent transitions in this visible probe region arise largely from metallic nanotubes, as evidenced by the impact on the linear absorption spectrum of selectively functionalizing metallic SWNTs as achieved by Strano *et al.*.[21] Transient absorption signals can arise from a modification of the transition oscillator strength or from a photoinduced shift of transition energies. A TA spectrum with maxima and minima spectrally aligned with those of the linear absorption indicate a change in oscillator strength; in contrast, energy-shifted transition energies yield maxima and minima correlated to the derivative of the linear absorption spectrum. Our measurements show (Fig. 2) that excitation of metallic SWNTs at energies well below the M_{11} first exciton energy produces transient responses at 1 ps delay very similar to that of excitation above the M_{11}. Apparently, even sub-M_{11} excitation modifies the oscillator strength of the M_{11} transitions for the metallic SWNTs. The excitation wavelength insensitivity demonstrates an equivalence in the resulting excited state at 1.0 ps delay for excitation above and

below the M_{11} in metallic SWNTs. Note the decrease in signal amplitude with increasing excitation wavelength (decreasing absorbed pulse energy) evident in Fig. 2(a). In Fig. 2(b), we show TA spectra at 1.0 ps delay for the case where the absorbed photon flux for the 1700 nm data is four times that at 430 nm, such that the total energy absorbed by the sample at each wavelength is approximately equal. The data show that the TA response in this visible probe region scales roughly linearly with the total energy absorbed by the SWNTs, independent of excitation wavelength. The excitation wavelength independence also suggests that metallic SWNTs contribute substantially to the optical density at each wavelength. Excitation at 430 and 1700 nm produces strikingly similar M_{11}-region TA spectra at 1.0 ps delay, considering that M_{11} interband transitions can be excited only by the 430 nm excitation.

The data clearly show a photoinduced absorption change at the M_{11} energies when exciting the sample at 1700 nm, a photon energy $\sim 1/3$ of the M_{11} energies. Our demonstrated transparency of semiconducting SWNTs below their S_{11} (see below) indicates that metallic SWNTs are indeed responsible for absorption at the lowest photon energies studied. Additionally, an M_{11} transient absorption response around 2 eV has been previously reported for sub-M_{11} excitation.[17] In this work, Korovyanko *et al.* ascribed the M_{11} photoresponse to "carrier heating," and suggested the behavior "shows that the primary photoexcitations in metallic SWNTs are free carriers."[17] However, the precise nature of the optical absorption by metallic SWNTs below the M_{11} transition is not clear. Although Drude-like absorption is not expected to be significant based on observed scattering lengths in metallic SWNTs, there is considerable evidence that free carriers in metallic SWNTs do in fact absorb at photon energies below the first interband transition.

Generally speaking, all measured linear absorption spectra of SWNTs exhibit a substantial "base," frequently attributed to the π-plasmon absorption,[11,31] upon which the features associated with interband transitions lie. The plasmon mode arises from a collective oscillation of the π electrons along the nanotube axis, and is analogous to the π-plasmon mode observed in graphite. Electron energy loss measurements show clearly that the tail of the π plasmon extends from the ~ 5 eV resonance energy to energies as low as 0.5 eV,[32,33] indicating that nonresonant excitation may play a role at low photon energies.[33] Low-energy π-plasmon absorption and the observed absorption below the M_{11} transition in metallic SWNTs have not yet been adequately addressed. Due to the merging and overlap of many S_{22} and M_{11} transition peaks, it is currently impossible to ascertain the precise shape and amplitude of the specific metallic and semiconducting SWNT components of the absorption spectrum. The PLE spectrum, however, indicates that the optical density of specific semiconducting SWNTs does not rise significantly as the photon energy increases above the S_{22} and S_{33} transitions [S_{33} not shown in Fig. 1(b)]. These observations, together with the TA response for metallic SWNTs scaling with total power absorbed, provide evidence that an electronic excitation in metallic SWNTs contributes significantly to the optical density at the excitation wavelengths studied.

Although direct transitions between linear-k bands are theoretically forbidden,[34] another possible mechanism for optical absorption at sub-M_{11} energies involves phonon-assisted (indirect) transitions between linear-k bands. For elevated temperatures, thermally excited electrons occupy states above the Fermi level in metallic SWNTs; these carriers may absorb low-energy photons in indirect, phonon-assisted intraband transitions along the linear-k band. Both interband and intraband indirect transitions require participation of a phonon, reducing the oscillator strength. Consistently, we observe only weak absorption in the low-energy, and largely featureless, region of the spectrum around 1700 nm.

To be complete, we must also consider the possibility of direct interband transitions between the linear-k bands. Ajiki and Ando have described these transitions as being unallowed,[34] but these calculations apply to perfect, infinite nanotubes. The solubilized HiPco SWNTs under study here are short and have reduced symmetry, perhaps permitting this formally unallowed transition to occur. Finally, we note that low-energy photoexcitation could occur across the 30–100 meV pseudogaps that are known to exist for metallic zigzag SWNTs.[30]

Interpretation of the ultrafast photoresponse of metallic SWNTs is made more challenging due to absorption both above and below the M_{11} transitions. We can gain some insight by considering a stepwise picture of the excited state evolution in metallic SWNTs, assuming metallic SWNTs account for 75% of the optical density at 430 nm excitation. For a total absorbed photon density of $2.5\times10^{14}\mathrm{cm}^{-2}$, we can compute the initial electron temperature from a value for the electronic specific heat of $\sim 7.1\ \mathrm{J\,kg^{-1}\,K^{-1}}$.[35] The areal density of SWNTs in our 1 mm pathlength cuvette is $\sim 1.6\times10^{-6}\ \mathrm{g/cm^2}$, and the pulse fluence absorbed by the free carriers is $\sim 8.6\times10^{-5}\ \mathrm{J/cm^2}$, yielding an initial electron temperature of ~ 7500 K. Rapid equilibration via phonon scattering will subsequently elevate the lattice temperature in the metallic SWNTs by ~ 75 K, owing to the larger heat capacity of the graphitelike lattice. Over the course of tens of picoseconds, the SWNTs will thermally equilibrate with the solvent, returning to ambient temperature. A photoinduced increase in the transition width would decrease the concentration of oscillator strength at transition peaks, and increase the oscillator strength in the wings of transitions, in agreement with the positive and negative $\Delta T/T_0$ values of Fig. 2. Lefebvre *et al.* have measured the temperature dependence of the linewidths for semiconducting SWNTs.[36] They observe a typical linewidth for ensembles of semiconducting SWNTs near 300 K of ~ 20 meV, and a broadening of $\sim 5\%$ for a 75 K temperature rise. We measure a thermal dissipation time for metallic SWNTs of ~ 100 ps (data not shown). This result stands in good general agreement with both a molecular dynamics simulation,[37] which found a typical thermal equilibration time of 75 ps for a SWNT-liquid system, and an experimental thermal dissipation result reported for colloidal gold nanocrystals.[38] Thus, the TA response we observe for the metallic SWNTs is consistent with a temperature-induced broadening of the M_{11} transitions. Korovyanko *et al.* observed a very fast (~ 200 fs) decay in the M_{11} signal for annealed films of SWNTs;[17] our data on dis-

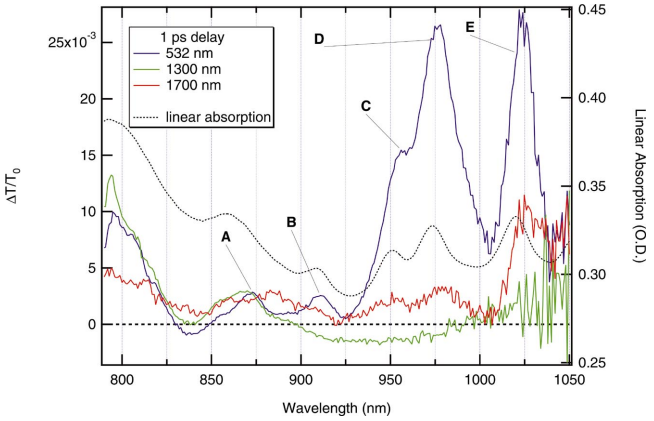

FIG. 3. (Color) Chirp-corrected transient absorption spectra for excitation at 532, 1300, and 1700 nm, acquired at 1.0 ps delay. Peaks *A*–*E* indicate peaks correlated to semiconductor SWNT emission peaks observed in the PL spectrum. The dotted line shows the linear absorption spectrum.

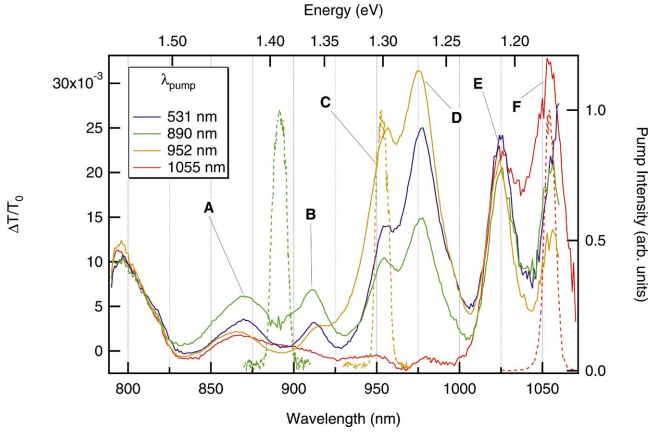

FIG. 4. (Color) Chirp-corrected transient absorption spectra for four pump wavelengths, acquired at 1.0 ps delay. Narrow peaks (dashed lines) show the pump spectra. Peaks *A*–*F* denote those features correlated to band-gap photoluminescence emission wavelengths.

persed SWNTs suggest that lattice heating determines the spectrally featured transient absorption data we observe for metallic SWNTs at 1 ps delay.

Turning now to the 790–1050 nm spectral region ("IR probe region"), Fig. 3 shows TA spectra acquired at 1.0 ps delay for pump wavelengths of 532, 1300, and 1700 nm. For HiPco SWNTs, this IR probe region includes M_{11} transitions for large-diameter metallic SWNTs,[39] as well as semiconducting S_{11} and S_{22} transitions.[8] In particular, for 532 nm cw laser excitation we observe photoluminescence peaks in this region assigned to specific semiconducting SWNTs at 873 nm (*A*), 911 nm (*B*), 955 nm (*C*), 980 nm (*D*), 1020 nm (*E*), and 1055 nm (*F*) [see Fig. 1(a), which includes (n,m) assignments]. We subsequently refer to these semiconducting SWNT spectral features by their assigned letters. Photoexcitation at 532 nm allows for excitation of all semiconducting tubes within our distribution, and we observe features in the TA spectrum corresponding to the S_{11} transitions for peaks *A*–*E* at 873, 912, 956, 975, and 1023 nm. Additional features are evident, for example at ~797 and ~850 nm, but we do not observe PL at these wavelengths. We therefore believe these peaks arise from S_{22} or M_{11} transitions.[39] In contrast to the response for 532 nm excitation, excitation at 1700 nm yields a spectrum of low-amplitude features. The absence of substantial TA peaks for B,C,D, and E indicate a near-zero excitation of these semiconducting SWNTs.

To investigate the transparency of semiconducting SWNTs more closely, we tuned the pump through this IR region, choosing excitation wavelengths of 531, 890, 952, and 1055 nm. Figure 4 shows TA spectra at 1.0 ps delay and the corresponding pump spectra (531 nm pump spectrum not shown). The TA spectra acquired at −5 ps have been subtracted to account for contributions of scattered pump light to the TA signal. We again hold the excitation level fixed at an absorbed photon density of 2.5×10^{14} cm^{-2}. As shown by the TA spectrum for $\lambda_{pump}=531$ nm, all semiconducting SWNTs in this region are photoexcited. All TA features remain when tuning to $\lambda_{pump}=890$ nm. The TA spectrum for $\lambda_{pump}=952$ nm shows a distinct decrease in the magnitude of peak *B*, with all longer wavelength peaks clearly present. Finally, tuning to $\lambda_{pump}=1055$ nm, the peaks at B,C, and D are virtually absent, while *E* and *F* remain clearly evident. We observe an apparent "up-conversion" excitation phenomenon, seen most clearly for excitation at 952 and 1055 nm. For $\lambda_{pump}=952$ nm, the peak *B*, centered at 912 nm, is excited in spite of being ~30 nm to the blue of the pump spectrum. And for $\lambda_{pump}=1055$ nm, the peak *E*, at 1023 nm, is excited. Since the 1055 nm excitation does not yield efficient excitation of even peak *D*, at 975 nm, we conclude that this up-conversion is limited in this case to an energy difference $\lesssim$75 meV. The full widths at half maximum (FWHMs) of our pump spectra are ~15 meV. Based on emission spectra, the FWHM of S_{11} transitions at room temperature has been reported as ~15–25 meV.[36] The up-conversion excitation likely reflects anti-Stokes phonon-assisted transitions. The TA spectra also show a resonance effect for peaks near the excitation wavelength, most notably for excitation wavelengths of 890 and 952 nm. The shape of the TA decay at the S_{11} provides another measure of population state filling. Figure 5 shows normalized transient bleach decays for the (6,5) SWNT ($\lambda_{probe}=975$ nm) as a function of excitation wavelength. While the curves for $\lambda_{pump}\leqslant990$ nm show similar bleach decays, the dynamics for $\lambda_{pump}\geqslant1150$ nm indicate a much faster transient response and exhibit small photoinduced absorption for delays between ~1 and 5 ps.

Emission from semiconducting SWNTs has not been reported for the S_{22} or higher transitions, indicating ultrafast relaxation to the S_{11} state. Correspondingly, we observe a very fast subpicosecond rise time of our TA signal, estimated to be $\lesssim$100 fs.[15] The rise time appears to be independent of nanotube type, and our measurements show no discernible increase in the absorption bleach rise time for excitation as high as 1.1 eV above the S_{11} of semiconducting SWNTs, indicating an energy loss rate as high as 5 eV/ps.[40] This carrier relaxation time is dramatically shorter than the radiative lifetime of 10 ns for the S_{22} state, as predicted for the (8, 0) SWNT by Spataru *et al.*;[41] the observed fast decay suggests that nonradiative processes dominate this relaxation, as

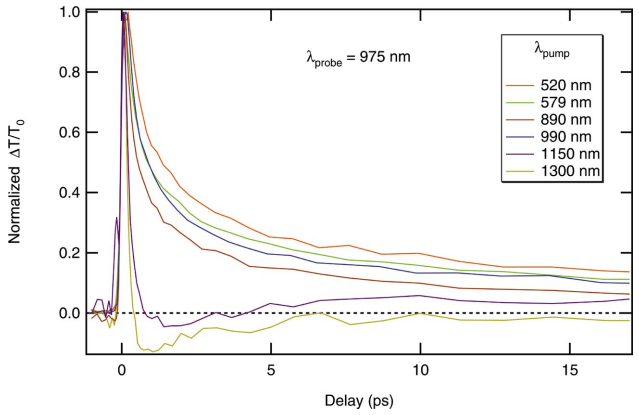

FIG. 5. (Color) Transient absorption dynamics measured at 975 nm for pump wavelengths varying between 520 and 1300 nm. Data have been normalized to the peak positive-going signal.

expected from the absence of emission from E_{22} and higher-lying levels. In agreement with Ostojic *et al.*,[12] we always observe a subpicosecond decay component in the TA signal. The subpicosecond component accounts for a significant fraction of the amplitude decay, and has been attributed to carrier-carrier scattering and Auger recombination.[9,15] Excitation density can play a role in ultrafast TA dynamics, due to the density dependence of carrier-carrier interactions.[42] Based on the 5 nm theoretical axial extent of the lowest-energy exciton wave function for the semiconducting (8, 0) nanotube,[41] our estimated excitation density of 300 excitons per micrometer of nanotube length is consistent with strong carrier-carrier interactions. We expect therefore that the effect of carrier-carrier interactions on our subpicosecond TA dynamics is dominant. As expected, the recombination rate slows as the carrier density decreases. Following the subpicosecond component, we observe multiexponential signal decay dynamics on the scale of ~1 ps to 1.8 ns (see Fig. 6). Spataru *et al.*[41] calculated a theoretical radiative lifetime of ~10 ns for the lowest bound exciton (S_{11}) of the (8, 0) semiconducting SWNT, based on the calculated transition dipole

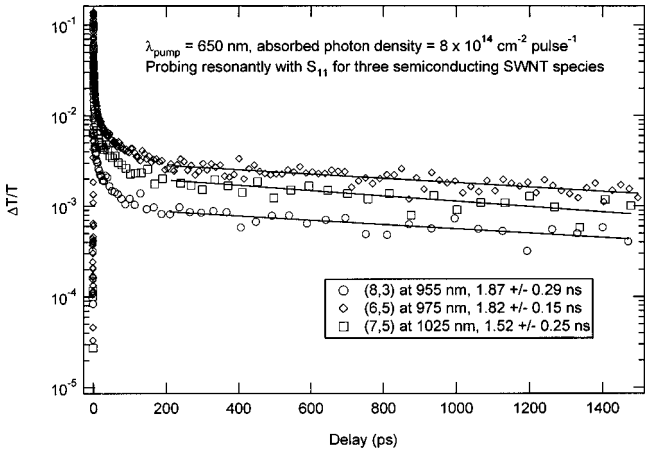

FIG. 6. Dynamics of the photoinduced bleach at the S_{11} for the (8,3), (6,5), and (7,5) semiconducting SWNTs, for $\lambda_{pump}=650$ nm and an absorbed photon density of 8×10^{14} cm^{-2}. Solid lines show single-exponential fits to long-lived components for $t_{delay}>200$ ps.

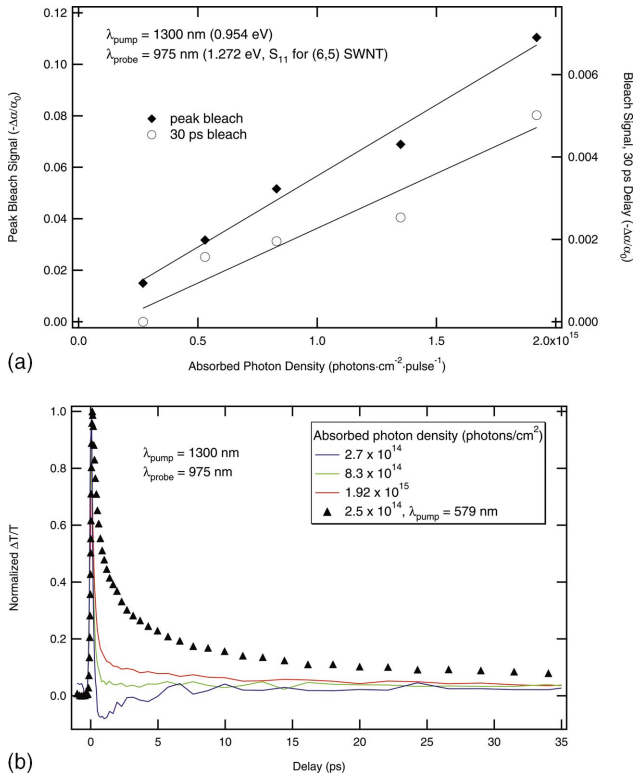

FIG. 7. (Color) (a) Intensity dependence of the photoinduced bleach signal at 975 nm, at the peak amplitude and at 30 ps delay, for 1300 nm excitation. The linear dependence indicates that the signal arises from linear absorption at the sub-band-gap energy, and not from two- or three-photon excitation. (b) Normalized transient absorption dynamics at 975 nm as a function of pump intensity at $\lambda_{pump}=1300$ nm. The triangles show the 975 nm dynamics for above-S_{11} excitation at $\lambda_{pump}=579$ nm.

strength. There have recently been estimates of luminescence lifetimes for dispersed SWNTs of ~100 (Ref. 43) and ~20 ps,[12] and in each case the deduced or observed carrier lifetime is much shorter than Spataru *et al.*'s predicted value. Surface interactions, tube-tube interaction effects, and/or mechanical stresses may reduce the carrier lifetime to the $\lesssim$100 ps time scale. Figure 6 shows a substantially slower decay component measured at the S_{11} energies for the (7,5), (6,5), and (8,3) semiconducting SWNTs, albeit at ~1% of the total signal amplitude. This long-lived TA signal, resolvable for the time regime when the carrier density has decreased sufficiently such that carrier-carrier recombination no longer dominates, may indicate S_{11} carrier lifetimes more than ten times larger than any previously reported for SWNTs. We note that Wang *et al.* have inferred a radiative lifetime of 110 ns for isolated SWNTs, based on combined measurements of time-resolved PL and quantum efficiency.[18] Alternatively, the long-lived TA component we observe could arise from a charge-separated state, or from slow thermal dissipation from photoheated SWNT bundles. Sufficiently sensitive time-resolved photoluminescence measurements would help in clarifying the source of the long lifetime.

Our intensity-dependent measurements indicate that the TA response of either metallic or semiconducting SWNTs to

sub-band-gap excitation does not result from multiphoton absorption. We consider here the (6,5) SWNT which shows a strong emission peak at 979 nm, resulting from the absorption peak near 975 nm. Figure 7(a) shows the intensity dependence of the TA response at 975 nm for excitation at 1300 nm. These measurements span the absorbed photon density range of $(2.7–19.0)\times 10^{14}$ cm^{-2}. This sub-band-gap excitation produces an intensity-dependent response at the (6,5) SWNT S_{11} absorption energy which is linear both at the peak and at a longer delay of 30 ps. The shape of the dynamical response is, however, not uniform with intensity over this range [Fig. 7(b)]. The 1300 nm excitation does not directly produce an S_{11} exciton population within the (6,5) SWNT (S_{11} at 975 nm, 1.27 eV). The brief photoinduced absorption ($\Delta T/T<0$) observed at the lowest excitation intensity may be due to excited state absorption by semiconducting SWNTs for which the S_{11} occurs at wavelengths longer than 1300 nm.[17] At higher intensities, thermal effects or a nonresonant bleach from photoexcited semiconducting SWNTs of lower S_{11} may dominate the photoresponse, overwhelming any excited state absorption. Note that the data shown in Fig. 5 are also consistent with a short-lived excited state absorption, revealed for sub-S_{11} excitation. An explanation based on thermal effects requires thermal contact between absorbing and nonabsorbing SWNTs, implying the existence of residual bundles or points of contact between SWNTs within samples of dispersed, solubilized SWNTs. The persistence of bundles within dispersed SWNT samples has been proposed or implied by some groups in recent reports,[13,16] and has also been contradicted.[18] The predominance of residual bundles is expected to decrease with more aggressive solubilization and centrifugation methods. A similar excited state absorption effect, for which the photoinduced bleach changes sign dynamically, has been previously reported.[15]

CONCLUSION

Transient absorption measurements utilizing a broadband probe have been conducted on dispersed SWNTs for spectral dependence at fixed delay, and also for temporal dependence at select spectral energies. Our detailed TA spectra for probe wavelengths in the range of 440–1050 nm show a clear correlation between the linear and transient spectra. Throughout the spectral region we have studied, the wavelengths of the peaks and valleys of the linear absorption spectrum match closely to those found in the transient bleach spectra for excitation above the first VHS transitions. The spectral alignment is consistent with a photoinduced change in the optical density centered at the M_{11} and S_{11} transitions of specific SWNT species, and not with a photoinduced shift in the positions of the energy levels. While both metallic and semiconducting SWNTs show transient bleaching at their M_{11} and S_{11} energies for excitation above these energies, metallic SWNTs uniquely exhibit a response to sub-M_{11} excitation energy. We attribute the TA response of metallic SWNTs, when pumped below the M_{11}, to a thermal effect involving the equilibration of the lattice and electronic heat capacities following absorption of the incident pulse. In contrast, semiconducting SWNTs show little or no response to sub-S_{11} excitation energy, in agreement with their expected zero DOS below S_{11}. In addition, we measure a long-lived excited state for three semiconducting SWNTs showing lifetimes exceeding 1.5 ns. Quenching of PL for semiconducting SWNTs cobundled with metallic SWNTs presents compelling evidence for efficient charge or energy transfer between nanotubes. Our studies provide a basis for time-resolved optical measurements of charge and energy transfer between specific SWNT species and coupled molecular or colloidal species.

Note added in proof. Since acceptance, we have become aware of work by Islam *et al.*[44] which presents measured nanotube absorption cross sections ~10 times smaller than our estimates. Islam's measurements indicate that the excitation density, and therefore the magnitude of thermal effects, may be overestimated in this report.

ACKNOWLEDGMENTS

The authors thank Yong-Hyun Kim, Shengbai Zhang, Thomas Gennett, and Matthew Beard for useful discussions. This work was supported by the U.S. Department of Energy (DOE) Solar Photochemistry program funded by the Office of Science, Office of Basic Energy Sciences, Division of Chemical Sciences, Geosciences, and Biosciences.

[1] A. C. Dillon, K. M. Jones, T. A. Bekkedahl, C. H. Kiang, D. S. Bethune, and M. J. Heben, Nature (London) **386**, 377 (1997).
[2] Q. H. Wang, A. A. Setlur, J. M. Lauerhaas, J. Y. Dai, E. W. Seelig, and R. P. H. Chang, Appl. Phys. Lett. **72**, 2912 (1998).
[3] W. B. Choi, D. S. Chung, J. H. Kang, H. Y. Kim, Y. W. Jin, I. T. Han, Y. H. Lee, J. E. Jung, N. S. Lee, G. S. Park, and J. M. Kim, Appl. Phys. Lett. **75**, 3129 (1999).
[4] B. Vigolo, P. Poulin, M. Lucas, P. Launois, and P. Bernier, Appl. Phys. Lett. **81**, 1210 (2002).
[5] J. N. Coleman, W. J. Blau, A. B. Dalton, E. Munoz, S. Collins, B. G. Kim, J. Razal, M. Selvidge, G. Vieiro, and R. H. Baughman, Appl. Phys. Lett. **82**, 1682 (2003).
[6] M. J. O'Connell, S. M. Bachilo, C. B. Huffman, V. C. Moore, M. S. Strano, E. H. Haroz, K. L. Rialon, P. J. Boul, W. H. Noon, C. Kittrell, J. Ma, R. H. Hauge, R. B. Weisman, and R. E. Smalley, Science **297**, 593 (2002).
[7] S. M. Bachilo, M. S. Strano, C. Kittrell, R. H. Hauge, R. E. Smalley, and R. B. Weisman, Science **298**, 2361 (2002).
[8] R. B. Weisman and S. M. Bachilo, Nano Lett. **3**, 1235 (2003).
[9] T. Hertel, R. Fasel, and G. Moos, Appl. Phys. A: Mater. Sci. Process. **75**, 449 (2002).
[10] M. Ichida, Y. Hamanaka, H. Kataura, Y. Achiba, and A. Nakamura, Physica B **323**, 237 (2002).
[11] J.-S. Lauret, C. Voisin, G. Cassabois, C. Delalande, P. Roussignol, O. Jost, and L. Capes, Phys. Rev. Lett. **90**, 057404 (2003).
[12] G. N. Ostojic, S. Zaric, J. Kono, M. S. Strano, V. C. Moore, R. H.

Hauge, and R. E. Smalley, Phys. Rev. Lett. **92**, 117402 (2003).
[13] L. Huang, H. N. Pedrosa, and T. D. Krauss, Phys. Rev. Lett. **93**, 017403 (2004).
[14] J.-S. Lauret, C. Voisin, G. Cassabois, P. Roussignol, C. Delalande, L. Capes, E. Valentin, A. Filoramo, and O. Jost, Semicond. Sci. Technol. **19**, S486 (2004).
[15] Y.-Z. Ma, J. Stenger, J. Zimmermann, S. M. Bachilo, R. E. Smalley, R. B. Weisman, and G. R. Fleming, J. Chem. Phys. **120**, 3368 (2004).
[16] I. V. Rubtsov, R. M. Russo, T. Albers, P. Deria, D. E. Luzzi, and M. J. Therien, Appl. Phys. A: Mater. Sci. Process. **79**, 1747 (2004).
[17] O. J. Korovyanko, C.-X. Sheng, Z. V. Vardeny, A. B. Dalton, and R. H. Baughman, Phys. Rev. Lett. **92**, 017403 (2004).
[18] F. Wang, G. Dukovic, L. E. Brus, and T. F. Heinz, Phys. Rev. Lett. **92**, 177401 (2004).
[19] M. J. Bronikowski, P. A. Willis, D. T. Colbert, K. A. Smith, and R. E. Smalley, J. Vac. Sci. Technol. A **19**, 1800 (2002).
[20] V. C. Moore, M. S. Strano, E. H. Haroz, R. H. Hauge, R. E. Smalley, J. Schmidt, and Y. Talmon, Nano Lett. **3**, 1379 (2003).
[21] M. S. Strano, C. A. Dyke, M. L. Usrey, P. W. Barone, M. J. Allen, H. Shan, C. Kittrell, R. H. Hauge, J. M. Tour, and R. E. Smalley, Science **301**, 1519 (2003).
[22] R. J. Ellingson, J. L. Blackburn, P. Yu, G. Rumbles, O. I. Micic, and A. J. Nozik, J. Phys. Chem. B **106**, 7758 (2002).
[23] V. I. Klimov and W. McBranch, Opt. Lett. **23**, 277 (1998).
[24] J. W. Mintmire, B. I. Dunlap, and C. T. White, Phys. Rev. Lett. **68**, 631 (1992).
[25] R. Saito, M. Fujita, G. Dresselhaus, and M. Dresselhaus, Phys. Rev. B **46**, 1804 (1992).
[26] N. Hamada, S. Sawada, and A. Oshiyama, Phys. Rev. Lett. **68**, 1579 (1992).
[27] J. W. Mintmire and C. T. White, Phys. Rev. Lett. **81**, 2506 (1998).
[28] C. T. White and T. N. Todorov, Nature (London) **393**, 49 (1998).
[29] R. Saito, G. Dresselhaus, and M. S. Dresselhaus, Phys. Rev. B **61**, 2981 (2000).
[30] M. Ouyang, J.-L. Huang, C. L. Cheung, and C. M. Lieber, Science **292**, 702 (2001).
[31] O. Jost, A. A. Gorbunov, W. Pompe, T. Pichler, R. Friedlein, M. Knupfer, M. Reibold, H.-D. Bauer, L. Dunsch, M. S. Golden, and J. Fink, Appl. Phys. Lett. **75**, 2217 (1999).
[32] T. Pichler, M. Knupfer, G. S. Golden, J. Fink, A. Rinzler, and R. E. Smalley, Phys. Rev. Lett. **80**, 4729 (1998).
[33] Z. M. Li, Z. K. Tang, H. J. Liu, N. Wang, C. T. Chan, R. Saito, S. N. Okada, G. D. Li, J. S. Chen, N. Nagasawa, and S. Tsuda, Phys. Rev. Lett. **87**, 127401 (2001).
[34] H. Ajiki and T. Ando, Physica B **201**, 349 (1994).
[35] L. X. Benedict, S. G. Louie, and M. L. Cohen, Solid State Commun. **100**, 177 (1996).
[36] J. Lefebvre, P. Finnie, and Y. Homma, Phys. Rev. B **70**, 045419 (2004).
[37] S. T. Huxtable, D. G. Cahill, S. Shenogin, L. Xue, R. Ozisik, P. Barone, M. Usrey, M. S. Strano, G. Siddons, M. Shim, and P. Keblinski, Nat. Mater. **2**, 731 (2003).
[38] M. B. Mohamed, T. S. Ahmadi, S. Link, M. Braun, and M. A. El-Sayed, Chem. Phys. Lett. **343**, 55 (2001).
[39] M. S. Strano S. K. Doorn, E. H. Haroz, C. Kittrell, R. H. Hauge, and R. E. Smalley, Nano Lett. **3** 1091 (2003).
[40] Measurement of the hot carrier relaxation dynamics in dispersed SWNTs is complicated by the typically high excitation densities used. The rise time of the bleach at the first interband transition energy for semiconducting SWNTs, containing information about the ultrafast carrier relaxation, is likely masked by ultrafast decay dynamics due to strong Auger recombination present at such high carrier densities.
[41] C. D. Spataru, S. Ismail-Beigi, L. X. Benedict, and S. G. Louie, Phys. Rev. Lett. **92**, 077402 (2004).
[42] V. I. Klimov, A. A. Mikhailovsky, D. W. McBranch, C. A. Leatherdale, and M. G. Bawendi, Science **287**, 1011 (2000).
[43] S. Lebedkin, K. Arnold, F. Hennrich, R. Krupke, B. Renker, and M. M. Kappes, in *Molecular nanostructures*, edited by H. Kuzmany, J. Fink, M. Mehring, and S. Roth, AIP Conf. Proc. No. 685 (AIP, Melville, NY, 2003), p. 230.
[44] M. F. Islam, D. E. Milkie, C. L. Kane, A. G. Yodh, and J. M. Kikkawa, Phys. Rev. Lett. **93**, 037404 (2004).